



This open access document is posted as a preprint in the Beilstein Archives at <https://doi.org/10.3762/bxiv.2020.113.v1> and is considered to be an early communication for feedback before peer review. Before citing this document, please check if a final, peer-reviewed version has been published.

This document is not formatted, has not undergone copyediting or typesetting, and may contain errors, unsubstantiated scientific claims or preliminary data.

Preprint Title Theoretical study of *NH* and *CH* acidities of toluidine isomers – dependence on their oxidation states

Authors Vladimir Lukes and Horst Hartmann

Publication Date 05 Oct 2020

Article Type Full Research Paper

Supporting Information File 1 SupplementaryMaterial-NHCH-acidity-VLHH.docx; 314.4 KB

ORCID® iDs Horst Hartmann - <https://orcid.org/0000-0002-4518-9295>

Theoretical study of *NH* and *CH* acidities of toluidine isomers – dependence on their oxidation states

Vladimir Lukeš^a, Horst Hartmann^{b*}

^aFaculty of Chemical and Food Technology, Slovak University of Technology in Bratislava, Radlinského
9, 812 37 Bratislava, Slovakia

^b Fakultät für Chemie und Lebensmittelchemie, Technische Universität Dresden, 01062 Dresden,
Germany

*corresponding author

Abstract

For the toluidine isomers, the amino group acidity represents a characteristic feature of these compounds in their electric neutral state. The *CH* acidity of methyl group is hidden under NH acidity. As demonstrated by theoretical calculations based on the quantum chemistry composite method G4 and Density functional theory, the transformation of toluidines into their mono- and bi-oxidised states significantly increases the acidity of methyl group. This study indicates that the presence or absence of these deprotonated species in reaction mixture will determine the *CN* or *CC* coupling toluidine products.

Keywords

Acidity of Oxidized States; Isodesmic Reaction; pK_a ; Anilinium Ion; M062X

Introduction

Thanks to the availability of a variety of modern analytic and physicochemical methods, such as the short-time spectroscopy [1], emission spectroscopy [2] and spectroelectrochemistry [3], it is possible to elucidate in the last time the mechanism of many organic chemical reactions and to indicate and characterize certain short-living species occurring thereby. The important role in this research play the highly-sophisticated quantum-chemical methods [4,5] which enable the theoretical description of molecular chemical and electronic structure, as well as the evaluation of thermodynamic properties. The theoretical calculations can be performed for the gas-phase and the role of solvent environment is standardly covered using the implicit solvent models [6].

Such an example of interesting problems in organic chemistry is the formation of acidic and basic species in the different electronic excited states. For these species, the corresponding dissociation constants and thermodynamic quantities differ mostly from the ones in the electronic ground states [7]. In this context of experimental and theoretical research activities, only few information exists on the estimation of such values for species in their reduced or oxidised states [8]. Similar to the electronic excited species, in the most cases such species are, owing to their open-shell nature, are highly reactive and are able to elude, therefore, their direct indication also. This situation will be more complicated if the corresponding acids or bases possess more than one acidic or basic centre in their molecular framework. This is the case, e.g. for the toluidines, which bear both at their amino and methyl groups protons which can be abstract principally by bases so that these compounds can exhibit, besides of their usual basic properties, also acidic properties. As far as these acidic properties are related to the protons at the *N*-atoms, they are called *NH*-acidity, whereas the basic properties which are related to the methyl groups are called *CH*-acidity.

Although the number of synthetic studies were focused on unravelling the products from oxidation of toluidine molecules under different conditions, the potential reactivity of oxidised toluidine isomers were discussed minimally. It is a lack of published experimental and theoretical knowledges about the reactive positions in the *N*-centred or *C*-centred species leasing to the *CN* or *CC* coupling

toluidine products. With respect to these facts, we decided to present the systematic theoretical analysis of parent and deprotonated toluidine and its oxidized species. The partial aims of this study are: (1) to calculate the optimal geometries of studied compounds in the gas-phase and two model environments; (2) to evaluate the reaction Gibbs free energies for selected reaction steps and (3) to estimate the corresponding acidity pK_a constants. The obtained theoretical trends and results will be confronted with the results published for various coupling reactions of toluidine isomers.

Results and Discussion

Thermodynamics of Toluidine Acid-Base Reaction

Aniline (ANH_2) as the simplest representative aromatic amine has basic as well as acidic, i.e. amphoteric, properties which can be quantified by the pK constants (**Scheme 1**) [9]. Comparing with ammonia, aniline solvated in water is a relative weak base. The corresponding experimental basicity pK_b constant of aniline is 9.4 [10] and ammonia in water is 9.2 [11]. On the other hand, the acidity constant of positive charged anilinium ion (pK_a), as conjugated acid of the base aniline at 298.15 K, in water is 4.6 and in DMSO is 3.7 (measured in aniline hydrochloride) [12]. Aniline is also a weak acid which can be deprotonated only by very strong bases, e.g. by lithium organyl compounds [13]. The available experimental pK_a for heterolytic dissociation of aniline to deprotonated anion (ANH^-) in DMSO is 30.6 [14]. The ammonia molecule represents an extremely weak acid due to the high pK_a value of 41.0 (in water) and of 38 (in DMSO) [15].

Scheme 1

From the thermodynamic point of view, the pK values are connected with the concentration equilibrium constants as a quantitative measure of the strength of an acid or base in solution. These equilibrium constants are related to the standard reaction Gibbs energy change for the acid-base reaction. For example, the pK_a value for heterolytic aniline dissociation can be calculated according to the following equation

$$pK_a = [\Delta G(\text{ANH}_2) - \Delta G(\text{H}^+) - \Delta G(\text{ANH}^-) + \Delta G_s(\text{ANH}_2) - \Delta G_s(\text{H}^+) - \Delta G_s(\text{ANH}^-) + RT \ln(24.46)] / [R T \ln 10] \quad (1)$$

where R is the universal gas constant. For the gas-phase, the commonly accepted value of gas-phase proton $\Delta G(\text{H}^+)$ is $-26.255 \text{ kJ mol}^{-1}$ [16]. The solvation Gibbs energies are denoted by down index s . The solvation of the proton is very important contribution that has direct influence on the stability and reactivity of solvated species. The contribution $RT \ln(24.46)$ reflects the change in the standard conditions from standard pressure 101.325 kPa to moles per liter. The solvation Gibbs energy $\Delta G_s(\text{H}^+)$ of proton is the Gibbs energy difference between a solvated proton $\Delta G(\text{H}^+)$ and the proton at rest under vacuum. The suggested theoretical value for water is $-1104.5 \text{ kJ mol}^{-1}$ and for DMSO is $-1123.8 \text{ kJ mol}^{-1}$ [17][18]. For the reference aniline and anilinium ion, the reaction Gibbs free energies for gas-phase and investigated solvent are collected in **Tab. 1**. The results for the gas-phase indicate that the dissociations aniline (ANH_2) as well as its conjugated acid (ANH_3^+) are endothermic. The G4 reaction Gibbs energies are $866.0 \text{ kJ mol}^{-1}$ for reaction **a** and $1513.8 \text{ kJ mol}^{-1}$ for reaction **b**. These energies are close to the values obtained from the reference M062x method, i.e. $850.4 \text{ kJ mol}^{-1}$ and $1505.9 \text{ kJ mol}^{-1}$. The inclusion of implicit solvent changes the thermic character of first acid base reaction. The comparison of gas-phase and IEF-PCM energies shows that the proton solvation represents the significant energy contribution and can determine final thermic character of investigated reactions. Although the maximal exothermic character exhibits the reactions in DMSO, the formation of ANH_3^+ in pure aprotic dimethyl sulfoxide is hypothetical. Comparing to the reaction **b**, the proton abstraction from aniline is not thermodynamically preferred. Similar to reference aniline, all three possible toluidine isomers (**o**-/**m**-/**p**- CH_3TNH_2) have basic as well as acidic properties. As it is depicted in **Scheme 2**, the proton abstraction from amino or methyl groups can be occurred in seven possible acid-base reactions.

Scheme 2

The mutual comparison of reaction G4 Gibbs energies for reactions **1**, **2** and **a**, **b** indicates minimal energy differences. The effect of methyl group position toward the amine group is also negligible, the maximal energy differences in solvents are up to the 6 kJ mol^{-1} . The results for reactions **4** and **5**

clearly show that the *CH* acidities of toluidines are, as expected, much weaker than their *NH* acidities and nearly independently from the substitution pattern. The energetically less preferred dissociation represents the proton abstraction from CH_3TNH^- anion (reaction No **5**). Interestingly, the *CH* acidities of zwitterion species CH_2TNH^+ in solvents are maximal for *ortho* isomer (reaction No. **3**) and it is comparable with the *NH* acidity of aniline (reaction No **2**). Next, the deprotonation of ammonium group in zwitterion species is also associated with the endothermic process (reaction No **2**). The comparable reaction Gibb's energies in solvents are indicated for *ortho* isomer. Finally, our calculations predict that the proton abstraction from $\text{CH}_2\text{TNH}_2^-$ is also possible. The calculated reaction Gibb's free energies for are ranged from 220.2 kJ mol⁻¹ to 234.5 kJ mol⁻¹ for DMSO and 234.4 kJ mol⁻¹ to 266.0 kJ mol⁻¹ for water.

The acid-base reactions of arylamines connected with the chemical oxidation of molecules are very often used in the preparation of poly-arylamines as materials with a high electric conductivity [18] or as starting materials for certain important organic dyes, such as Mauveine or Fuchsine [19]. It is from some practical interest to know that the *NH* and *CH* acidities of toluidines depend not only from the substitution position of their methyl groups at the aromatic ring but also from the oxidation state of the corresponding compounds. In this context, four possible acid-base reactions (Nos. **8**, **9**, **10** and **11**) initiated upon the electron abstractions were theoretically investigated for toluidines (see **Scheme 3** and **Fig. 1S**). The theoretical results collected in **Tab. 1** and in **Tab. 1S** as well as depicted for water in Scheme 3 show that the *NH* and *CH* acidities of toluidine are increased by going from the mono oxidised species (CH_3TNH^+) to their bis-oxidised species (HNTCH_3^{2+}). For the *N*-centred cations (CH_3TNH^+) and the *N*-centred radicals ($\text{CH}_3\text{TNH}^\cdot$) two different electronic structures are possible for each isomeric compound. The π -type structure has non-occupied valence orbitals at the *N*-atom which are in conjugation with remaining aromatic π -electrons. The second structure has well separated single occupied valence orbitals at the *N*-atom (σ -type). The quantum chemical calculations follow that in both cases the π -type species are more stabilised than the σ -type species

(see **Fig. 2S**). This is in agreement with calculations performed by other authors for various nitrogen-centred radicals [20].

Scheme 3

Theoretical pK_a Values of Toluidine Oxidation States

The theoretical pK_a values evaluated from quantum chemical results (see Eq. 1) can lead to the values different from experiment (see **Tab. 2S**). This error is connected with the insufficient description of solvent effects using the implicit model. Next, the PCM models is employed to calculate solvation energies in high accuracy, it requires parametrization of the shape and size of the dielectric cavity of a molecule [21]. Unfortunately, computational works reported to date rarely involved extensive parametrization for radical species or charged states. To improve the reliability of theoretical pK_a values, the approach based on the isodesmic reaction is applied [22]. In this work, we have used the available experimental pK_a data for aniline, anilinium ion and aniline cation radical in DMSO and water (see **Tab. 2**). In case of aniline dissociation in pure water, the reliable experimental pK_a value is not available in literature. Therefore, we have decided to estimate the reference value from experimental value for DMSO and theoretical values for water and DMSO. If we suppose the linear dependence, the estimated value is 34.5 ($30.6 \times 32.7 / 29.1$).

The theoretically predicted pK_a values for selected acid-base reaction are collected in **Tab. 2**. Although the calculated reaction Gibb's free energies for the reaction **a** in solvents predict the thermodynamic instability of anilinium ion, the experimental pK_a value of 4.6 indicates the opposite character. The reaction Gibb's free energy should be positive. Based on the isodesmic reaction approach, the predicted pK_a values for the dissociation of **o-/m-CH₃TNH₂** and **p-CH₃TNH₂⁺** are 4.8, 4.7 and 5.3, respectively. The experimental data for *ortho*, *meta* and *para* toluidine (conjugated acid) in aqueous solution are 4.4 [23], 4.7 and 5.1 [11]. The differences between the theoretical and experimental values indicate that the ortho effect in toluidine isomer is slightly overestimated in used calculation model.

The experimental values for reaction **b** were used for the pK_a calculations of reactions Nos. **2** to **7**. In agreement with the calculated reaction Gibb's free energies in solvents, the highest pK_a values are connected with the proton abstraction from methyl group (see reaction No. **4**). The pK_a values for DMSO are between 43.7 to 47.7 and for water are 46.9 and 47.1. These high values for methyl group acidity are in agreement with the results for toluene. The electron-donating methyl group in toluene undergoes deprotonation only with very strong bases, its pK_a is estimated to be approximately 41 [14]. On the other hand, the acidities of zwitterion species $\text{CH}_2\text{TNH}_3^+$ in water or DMSO/water mixture for reaction No. **6** are very high. The lowest pK_a values were found for meta isomers, i.e. 1.4 for DMSO and 4.7 for water. The pK_a values for reactions of cations and dications (**8** to **10**) were evaluated with respect to the experimental values of aniline cation reaction **c**. Remarkably, for the mono-oxidised species, the *NH* and *CH* acidity are nearly the same in all solvents, but the *CH* acidity is slightly larger than the *NH* acidity. Therefore, the formation of a *N*-centred radical $\text{CH}_3\text{TNH}\cdot$ is slightly lesser favoured over the formation of a corresponding *C*-centred radical CH_2TNH_2 . It seems that the maximal pK_a values for reactions No. **8** and **9** are connected with *para* isomers. The available experimental pK_a value for *para* isomer in DMSO (reaction No. **8**) is 8.3 what is well interpreted by theoretical value of 7.3 [8]. According to the calculated most negative reaction Gibb's energies for reaction **10** and **11**, very strong acidities are predicted for bi-oxidised states. In general, the *o*- and *p*-isomers in the bi-oxidised state are some more stabilised as their *m*-isomer.

Oxidation States and Reactivity of Toluidine

The calculated acidities of toluidine in their different oxidation states (Tab. 2) show that the toluidine radical cations $\text{CH}_3\text{TNH}_2^+$ as primary species generated by the oxidation of toluidines, can be deprotonated both at their NH_2 and CH_3 moieties. This deprotonation leads to the transformation into *N*-centred radical $\text{CH}_3\text{TNH}\cdot$ and *C*-centred radical CH_2TNH_2 . On the other hand, the toluidine dications $\text{CH}_2\text{TNH}_2^{2+}$ as secondary species generated by the oxidation of toluidines can be deprotonated exclusively at their methyl moieties and transformed thereby into *C*-centred cationic

species $\text{CH}_2\text{TNH}_2^+$. Owing to the highly negative pK_a values of reaction **10**, the cationic species $\text{CH}_2\text{TNH}_2^+$ can be formed also directly from the radical cations $\text{CH}_3\text{TNH}_2^{\bullet+}$ in course of a so-called proton-coupled electron transfer (PCET) process [25]. We would like to note that under usual pH -conditions ($0 < \text{pH} < 9$), which are applied in course of the oxidation of aniline and its derivatives, there is no change for the formation of the dicationic species $\text{CH}_3\text{TNH}_2^{2+}$, although certain authors argue for its existence [25, 26, 27].

From the data derived follow, that by starting with *p*-toluidine (**Scheme 4**), an oxidatively mediated coupling of the *N*-centred radicals $\text{p-CH}_3\text{TNH}^\bullet$, e.g. with a further *p*-toluidine, is expected. Indeed, such a coupling occurs at the *N*-atom and gives rise to the formation of a coupling product of the general structure **D**₁. This compound is able to react with a further *p*-toluidine molecule yielding the so-called BARSILOWSKY's base **T**₁ [26]. In the second case, namely by reaction of the radical cation $\text{CH}_3\text{TNH}_2^{\bullet+}$, an oxidatively mediated coupling with *p*-toluidine is expected to occur at the CH_2 moiety and gives rise to the formation of a coupling product of the general structure **D**₂ [27]. This compound can subsequently be transformed by further oxidation into the azomethine compound **D**₃, which is able to yield, e.g. by further reaction with aniline, Fuchsine [28].

Scheme 4

According to **Scheme 5**, in a similar transformation of *o*-toluidine into its radical cation $\text{o-HNTCH}_3^{\bullet+}$ a deprotonation at its *N*-atom yielding the *N*-centred radical $\text{o-CH}_3\text{TNH}^\bullet$ can occur, whereas by the transformation of *o*-toluidine into its di-cationic species $\text{o-CH}_3\text{TNH}_2^{2+}$ a deprotonation at the methyl moiety occurs. In course of a corresponding PCET process, the *C*-centred radical $\text{o-CH}_2\text{TNH}_2^\bullet$ is formed directly also from the radical cation $\text{o-CH}_3\text{TNH}_2^{\bullet+}$. The *N*-centred radical $\text{o-CH}_3\text{TNH}^\bullet$ is able to couple with a parent *o*-toluidine at its *N*-atom. It gives rise to the formation of the dimer **D**₄ from which the quinone iminium salts **D**₅ is formed [29]. The *C*-centred cation $\text{o-CH}_2\text{TNH}_2^+$ is highly reactive [30] and can be transformed either by reaction with certain nucleophiles into the adducts **X**₂ or by reaction with further *o*-toluidine or aniline (ANH_2), *via* the dimer **D**₆, into the acridines **D**₇ [31] or the Chrysaniline **D**₈ [32].

Scheme 5

Although the oxidation of *m*-toluidine is also studied rather intensively, in contrast to the oxidation of *o*- and *p*-toluidine, there is only less information on the structure of products and on the mechanism of their formation. Thus, it was stated that by the electrochemical oxidation of *m*-toluidine, performed in acidic solution, in course of a *CN* coupling reaction a polymer is formed its structure **D₁₀** is similar to the one which is formed by the oxidation of aniline (**Scheme 6**) [33]. Moreover, similar to the aniline oxidation certain intermediates, such as the 1,4-phenylenediamine derivative **D₉** and the quinoneimine **D₁₀** with *n* = 1 [34], and the corresponding benzidine derivatives **D₁₁** and **D₁₂** [35] have been identified. Moreover, similar to the aniline oxidation, a corresponding azobenzene derivative, which can be formed from the radical species **m-CH₃TNH·** in course of a *NN* coupling, has been identified also. However, there is no information at yet on the formation of products which could be generated from the zwitterion product **m-CH₂TNH₂⁺** formed by a deprotonation at the methyl group in *meta*-position.

Scheme 6

Conclusion

In this theoretical study, we have suggested possible acid-base reaction steps occurring during the oxidation of toluidine isomers. The reaction Gibb's energies were calculated using G4 and M062x approaches for the gas-phase, water and dimethylsulfoxid environments. The theoretical p*K_a* values were evaluated for mono- and bi-cationic states using the isodesmic reaction approach with respect to the reference experimental data available for the aniline molecule. The comparison of these values showed that the transformation of toluidines into oxidised states significantly increases the acidity of methyl group. This study indicates that the presence or absence of these deprotonated species in reaction mixture will determine the *CN* or *CC* coupling toluidine products. The qualitatively

similar theoretical results were also obtained using the reference density functional theory and M062x functional.

Experimental

Computational methods

The quantum chemical calculations based on the Density Functional Theory were performed using the Minnesota M062x hybrid functional [36] and 6-311++G** basis set of atomic orbitals [37]. First the optimal geometries of the studied species were found in gas-phase and these optimal geometries were used as the starting geometries for the calculations using Gaussian-4 theory [38]. This theory involves the introduction of an extrapolation scheme for obtaining basis set limit Hartree-Fock energies and it was developed for the calculations of thermochemical properties. The solvent effects contributions in dimethylsulfoxide (DMSO) and in water (WAT) were described using the integral equation formalism version of PCM (IEF-PCM) [39]. Frequency analysis showed no imaginary frequencies confirming the real geometry of the energy minima. All Gibb's free energies were estimated for temperature $T = 298.15$ K and pressure $p = 101325$ Pa. These thermodynamic energies are calculated from the combination of energy contributions from various B3LYP and *ab initio* energies. All calculations were carried out using the Gaussian 16 program package [40]. The molecules and spin densities were visualised using the Molekel program package [41].

Supporting Information

Supporting Information File 1: Additional calculated data.

Funding

The authors gratefully acknowledge to Slovak Research and Development Agency (APVV-15-0053). We are grateful to the HPC centre at the Slovak University of Technology in Bratislava, which is a part

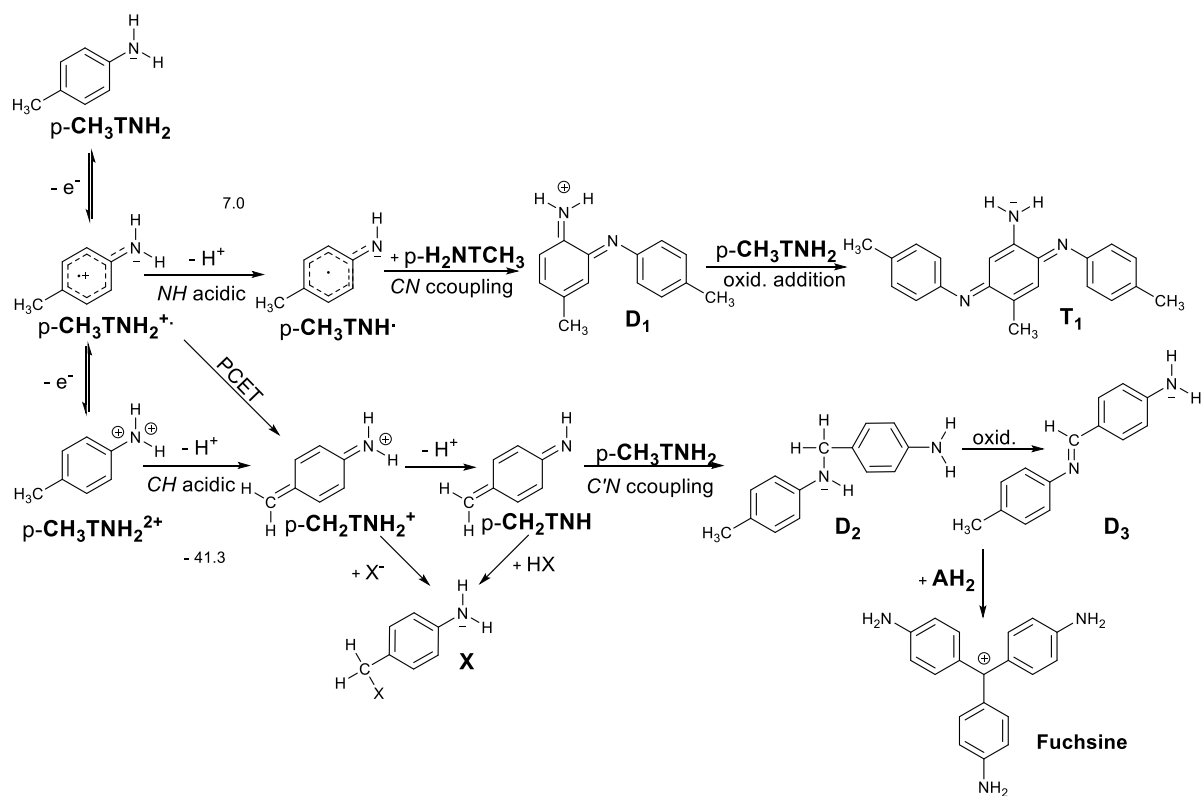
of the Slovak Infrastructure of High Performance Computing (SIVVP project, ITMS code 26230120002, funded by the European region development funds, ERDF) for the computational time and resources made available.

References

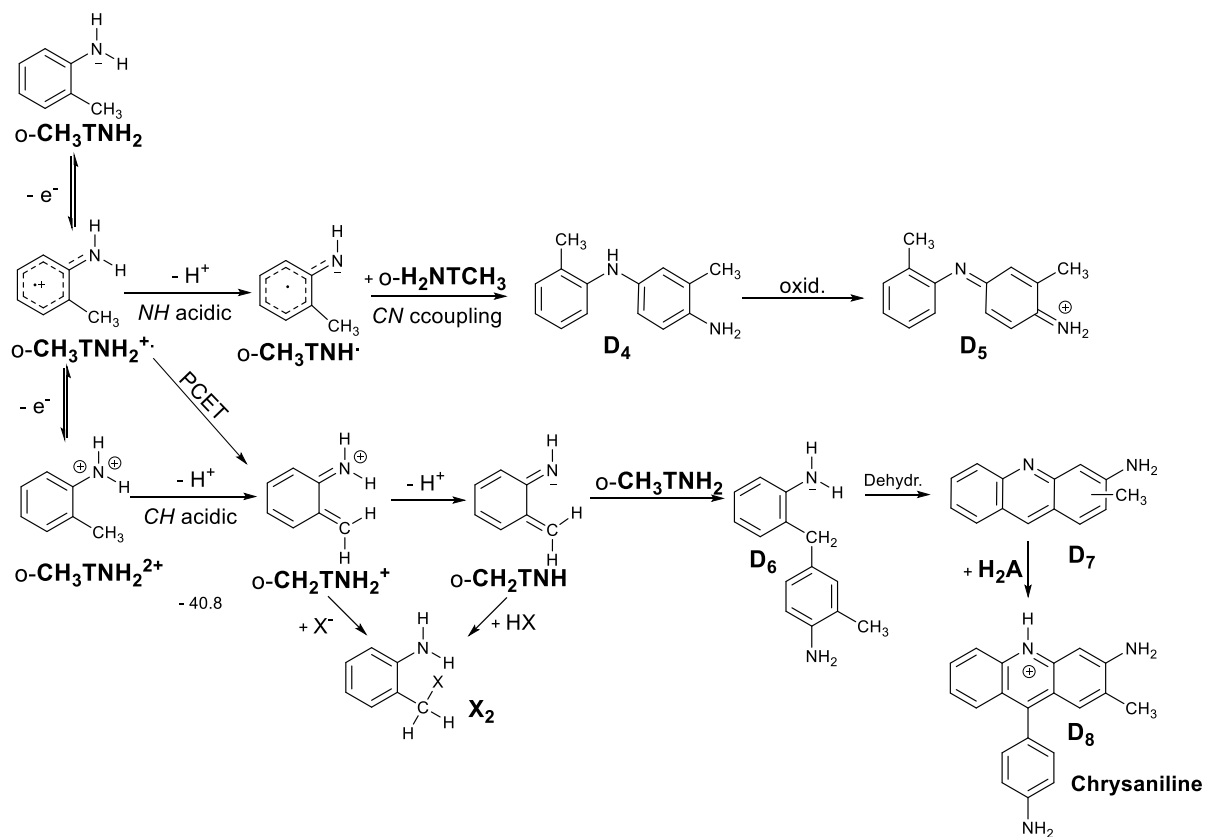
- [1] Maiuri, M. ; Garavelli, M.; Cerullo G. *J. Am. Chem. Soc.* **2020**, *142*, 3–15 references given therein; Oliver T. A. *R. Soc. Open Sci.* **2018**, *5*, 171425 (21 pages).
- [2] Valeur, B. *Molecular Fluorescence Principles and Applications*; VCH-Wiley: Weinheim, Germany, 2001; Lakowicz, J. R. *Principles of Fluorescence Spectroscopy*, 3rd ed.; Springer: New York, USA, 2006; Sauer, M.; Hofkens, J.; Enderlein J. *Handbook of Fluorescence Spectroscopy and Imaging; From Ensemble to Single Molecules*; Wiley-VCH: Weinheim, Germany, 2011.
- [3] Mortimer, R. *Encyclopedia of Spectroscopy and Spectrometry* **2017**, *4*, 160–171; 172–177; Rapta, P.; Dmitrieva, E.; Popov, A. A.; Dunsch, L. *Org. Electrochem.* **2016**, 169–190; Low, P. J.; Bock, S. *Electrochim. Acta* **2013**, *110*, 681–692; Venturi, M. Spectroelectrochemistry, in *The Exploration of Supramolecular Systems and Nanostructures by Photochemical Techniques, Lecture Notes in Chemistry*, Ceroni, P. Eds.; Springer Science+Business Media B.V., 2012; Vol. 78; Dunsch, L. *J. Solid State Electrochem.* **2011**, *15*, 1631–1646; Nekrasov, A. A.; Vannikov, A. V. *Russ. J. Electrochem.* **2011**, *47*, 1–14; Kaim, W.; Fiedler, J. *Chem. Soc. Rev.* **2009**, *38*, 3373–3382; Toma, H. E.; Araki, K. *Current Org. Chem.* **2002**, *6*, 21–34; Plieth, W.; Wilson, G. S.; De La Fe, C. G. *Pure Appl. Chem.* **1998**, *70*, 1395–1414.
- [4] Parr, R. G.; Yang, W. *Density-Functional Theory of atoms and molecules*, Oxford University Press, New York, 1989.
- [5] Zhao, Y., Schultz, N. E.; Truhlar, D. G. *J. Chem. Theory and Comput.* **2006**, *2*, 364–382.
- [6] Guerard, J. J.; Arey, J. S. *J. Chem. Theory Comput.* **2013**, *9*, 5046–5058.
- [7] Tolbert, L. M. *Acc. Chem. Res.* **2002**, *35*, 19–27.
- [8] Bordwell, J. F.; Zhang, X.-M.; Cheng, J.-P. *J. Org. Chem.* **1993**, *58*, 6410–6416; Jonsson, M.; Lind, M.; Eriksen, T. E.; Merenyi, G. *J. Am. Chem. Soc.* **1994**, *116*, 1423–1427.
- [9] Bordwell, F. G.; Algrim, D. J. *J. Am. Chem. Soc.* **1988**, *110*, 2964–2968.
- [10] Kim, H.-S.; Chung, T. D.; Kim, H. *J. Electroanal. Chem.* **2001**, *498*, 209–215.
- [11] Perrin, D. D. *Dissociation constants of organic bases in aqueous solution*; IUPAC Chem. Data Ser: Suppl; Butterworth: London, United Kingdom, 1972.
- [12] Kelley, C. P.; Cramer, C. J.; Truhlar, D. G. *J. Phys. Chem. B* **2006**, *110*, 16066–16081.
- [13] Bismuto, A.; Delcaillau, T.; Muller, P.; Morandi, B. *ACS Cat.* **2020**, *49*, 4630–4639.
- [14] Ripin, D. H. B. pKa; In *Practical Synthetic Organic Chemistry: Reactions, Principles, and Techniques*; Caron S. Eds.; John Wiley & Sons, 2011, 771–803; Rezende, M. C. J. *Braz. Chem. Soc.* **2001**, *12*, 73–80.
- [15] Bartmess, J. E. *J. Phys. Chem.* **1994**, *98*, 6420–6424.

- [16] Trummal, A.; Rummel, A.; Lippmaa, E.; Burk, P.; Koppel, I. A. *J. Phys. Chem. A* **2009**, *113*, 6206–6212.
- [17] Tissandier, M. D.; Cowen, K. A.; Feng, W. Y.; Gundlach, E.; Cohen, M. H.; Earhart, A. D.; Coe, J. V.; Tuttle, T. R. *J. Phys. Chem. A* **1998**, *102*, 7787–7794.
- [18] Mortimer, R. J. *Chem. Soc. Rev.* **1997**, *26*, 147–156; Syed, A. A.; Dinesan, M. K. *Talanta* **1991**, *38*, 815–835.
- [19] Cooksey, C. J.; Dronsfield, A. T. *Educ. Chem.* **2010**, *47*, 18–21; Ihmels, H. *Beilstein J. Org. Chem.* **2019**, *15*, 2798–2800.
- [20] Hioe, J.; Šakić, D.; Vrček, V.; Zipse, H. *Org. Biomol. Chem.*, **2015**, *13*, 157–169.
- [21] Tomasi, J.; Persico, M. *Chem. Rev.* **1994**, *94*, 2027–2094.
- [22] Sastre, S.; Casasnovas, R.; Muñoz, F.; Frau, J. *Phys. Chem. Chem. Phys.* **2016**, *18*, 11202–11212.
- [23] Huyskens, P.; Mullens, J.; Gomez, A.; Tack, J. *Bull. Soc. Chim. Belg.* 1975, *84*, 253–262.
- [24] Weinberg, D. R.; Gagliardi, C. J.; Hull, J. F.; Murphy, C. F.; Kent, C. A.; Westlake, B. C.; Paul, A.; Ess, D. H.; McCafferty, D. G.; Meyer, T. J. *Chem. Rev.* **2012**, *112*, 4016–4093; Hammes-Schiffer, S.; Stuchebrukhov, A. A. *Chem. Rev.* **2010**, *110*, 6939–6960; Hang, M.; Huynh, V.; Meyer, T. J. *Chem. Rev.* **2007**, *107*, 5004–5064; Cukier, R. I. *J. Phys. Chem.* **1996**, *1000*, 15428–15443.
- [25] Peng, K.-S.; Zeng, Q.-L.; Zhang, W.; *Heheng Huaxue* **2010**, *18*, 239–241; Plater, M. J. *J. Chem. Res.* **2014**, *38*, 351–355.
- [26] Kouznetsov V.; Vargas Méndez, L. Y.; Sortino, M.; Vásquez, Y.; Gupta, M. P.; Freile, M.; Enriz, R. D.; Zacchino, S.A. *Biorg. Med. Chem.* **2008**, *16*, 794–809.
- [27] Fischer, O. Verfahren zur Herstellung des Triphenylmethans und seiner Abkömmlinge, D.E. Patent 1,6710, Jan 5, 1882.
- [28] Lu, W.; Xi, C. *Tetrahedron Lett.* **2008**, *49*, 4011–4015; Bardajee, G. R. *Beilstein J. Org. Chem.* **2011**, *7*, 135–144.
- [29] Saunthwal, R. K.; Patel, M.; Verma, A. K. *Org. Lett.* **2016**, *18*, 2200–2203.
- [30] Ullmann, F. *Ber. Dtsch. Chem. Ges.* **1903**, *36*, 1017–1027.
- [31] Amos, S. G. E; Garreau, M.; Buzzetti, L.; Waser, J. *Beilstein J. Org. Chem.* **2020**, *16*, 1163–1187; BASF, Verfahren zur Darstellung von unsymmetrischen Diaminodiphenylakridinen, D.E. Patent 94,951, April 4, 1897; BASF, Verfahren zur Darstellung von unsymmetrischen Diaminodiphenylakridinen, D.E. Patent 102,072, 1899.
- [32] Sayyah, S. M.; Shaban, M.; Rabia, M. *Adv. Polymer Techn.* **2018**, *37*, 126–136 and the references given therein.
- [33] Hand, R. L.; Nelson, R. F. *J. Electroanal. Soc.* **1978**, *125*, 1059–1069.

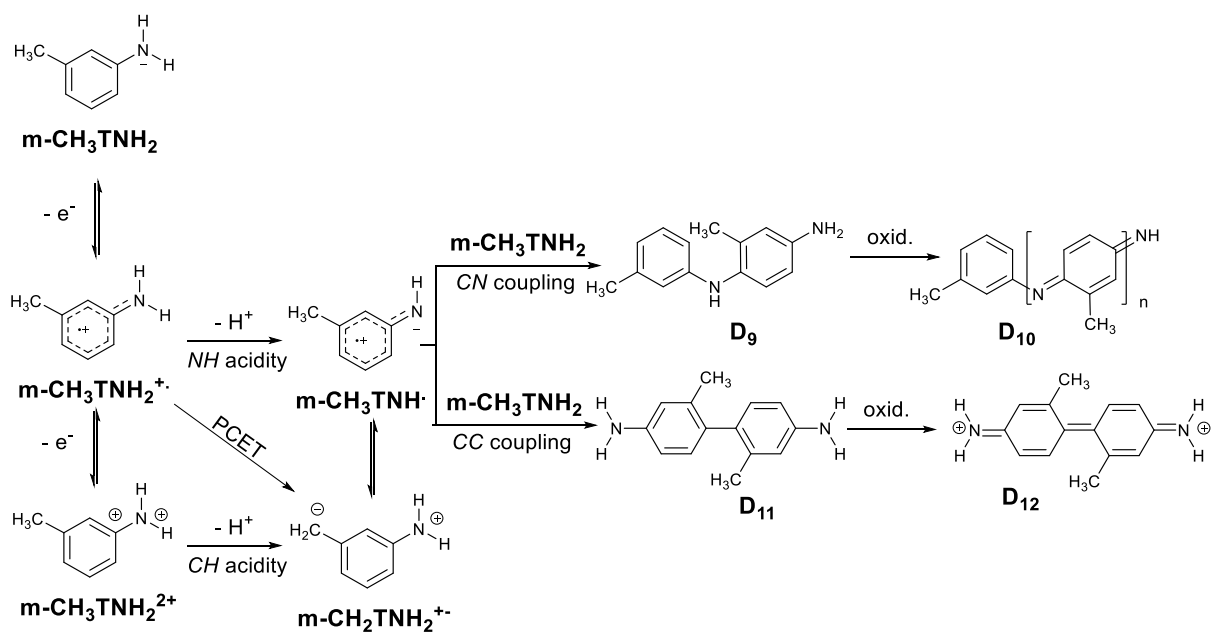
- [34] Desidero, P. G.; Lepi, L.; Heimler, P. *J. Electroanalyt. Chem. Interfacial Electrochem.* **1974**, *52*, 93–103.
- [35] Sharma, L.R.; Manchanda; A.K.; Singh, G.; Verma, R.S. *Electrochim. Acta* **1982**, *27*, 223 – 233.
- [36] Zhao, Y., Truhlar, D. G. *Acc. Chem. Res.*, **2008**, *41*, 157–167.
- [37] Hariharan; P. C.; Pople, J. A. *Theor. Chim. Acta.* **1973**, *28*(3), 213–222
- [38] Redfern, L.A.; Raghavachari P. C. *J. Chem. Phys.* **2007**, *126*, 084108 (12 pages).
- [39] Mennucci, B.; Tomasi, J. *J. Chem. Phys.* **1997**, *106*, 5151–5158; Mennucci, B.; Cancès, E.; Tomasi, J. *J. Phys. Chem. B* **1997**, *101*, 10506–10517; Tomasi, J.; Mennucci, B.; Cancès, E. *J. Mol. Struct. (THEOCHEM)* **1999**, *464*, 211–226; Chipman, D. M. *J. Chem. Phys.* **2000**, *112*, 5558–5565; Cancès, E.; Mennucci, B. *J. Chem. Phys.* **2001**, *114*, 4744–4745
- [40] Gaussian 16, Revision B.01, Gaussian, Inc., Wallingford CT, 2016.
- [41] Flukiger, P.; Luthi, H. P.; Sortmann, S.; Weber J. *Molekel* (version 5.4.0.8), Swiss National Supercomputing Centre, Manno, Switzerland, 2009.



Scheme 4



Scheme 5



Scheme 6

Table 1. Reaction G4 Gibb's free energies for selected acido-basic steps calculated for the gas-phase and solvents (energies in kJ mol⁻¹).

Reaction No.	Acid-base reaction	G4			G4			G4			
		gas			DMSO			water			
a	$\text{ANH}_3^+ \rightarrow \text{ANH}_2 + \text{H}^+$		866.0			-38.4				-17.1	
b	$\text{ANH}_2 \rightarrow \text{ANH}^- + \text{H}^+$		1513.8			176.4				193.7	
c	$\text{ANH}_2^{*+} \rightarrow \text{ANH}^* + \text{H}^+$		927.8			1.1				22.0	
		<i>ortho</i>	<i>meta</i>	<i>para</i>	<i>ortho</i>	<i>meta</i>	<i>para</i>	<i>ortho</i>	<i>meta</i>	<i>para</i>	
1	$\text{CH}_3\text{TNH}_3^+ \rightarrow \text{CH}_3\text{TNH}_2 + \text{H}^+$	868.9	871.5	874.7	-35.0	-37.6	-34.6	-16.0	-16.1	-13.3	
2	$\text{CH}_3\text{TNH}_2 \rightarrow \text{CH}_3\text{TNH}_2^- + \text{H}^+$	1509.0	1497.5	1520.3	177.8	179.5	183.6	194.9	196.9	195.9	
$\Delta(G_1 - G_2)$		-640.1	-626.0	-645.6	-212.8	-217.1	-218.2	-210.9	-212.9	-209.2	
3	$\text{CH}_3\text{TNH}_3^{*+} \rightarrow \text{CH}_2\text{TNH}_3^{*+} + \text{H}^+$	1143.8	1183.3	1197.7	186.6	205.0	211.6	204.8	226.0	208.5	
4	$\text{CH}_3\text{TNH}_2 \rightarrow \text{CH}_2\text{TNH}_2^- + \text{H}^+$	1579.2	1560.2	1601.4	251.4	252.2	274.0	268.7	269.4	269.7	
5	$\text{CH}_3\text{TNH}^- \rightarrow \text{CH}_2\text{TNH}_2^{2-} + \text{H}^+$	1971.2	1952.9	1964.2	308.1	292.7	320.4	322.2	306.9	339.7	
$\Delta(G_2 - G_4)$		-70.2	-62.7	-81.1	-73.8	-72.5	-73.8	-73.6	-72.7	-90.4	
6	$\text{CH}_2\text{TNH}_3^{*+} \rightarrow \text{CH}_2\text{TNH}_2^- + \text{H}^+$	1304.4	1248.4	1278.4	29.8	9.5	27.8	47.9	27.4	47.9	
7	$\text{CH}_2\text{TNH}_2^- \rightarrow \text{CH}_2\text{TNH}^{2-} + \text{H}^+$	1901.0	1890.2	1883.2	234.5	220.2	230.1	248.4	234.4	266.0	
$\Delta(G_6 - G_7)$		-596.6	-641.7	-604.8	-204.7	-207.0	-218.1	-200.5	-207.0	-218.1	

Table 1 (continued). Reaction G4 Gibb's free energies for selected acido-basic steps calculated for the gas-phase and solvents (energies in kJ mol⁻¹).

Reaction No.	Acid-base reaction	G4			G4			G4		
		gas			DMSO			water		
		<i>ortho</i>	<i>meta</i>	<i>para</i>	<i>ortho</i>	<i>meta</i>	<i>para</i>	<i>ortho</i>	<i>meta</i>	<i>para</i>
8	$\text{CH}_3\text{TNH}_2^{2+} \rightarrow \text{CH}_3\text{TNH}^+ + \text{H}^+$	937.9	939.5	943.1	2.7	4.6	5.6	23.6	25.4	23.6
9	$\text{CH}_3\text{TNH}_2^{2+} \rightarrow \text{CH}_2\text{TNH}_2^+ + \text{H}^+$	937.2	932.1	943.3	-0.6	2.0	4.9	20.3	22.7	20.3
$\Delta(G_8 - G_9)$		0.7	7.4	-0.2	3.3	2.6	0.6	3.3	2.7	3.3
11	$\text{CH}_3\text{TNH}_2^{2+} \rightarrow \text{CH}_3\text{TNH}^+ + \text{H}^+$	285.8	312.2	295.1	-255.5	-203.5	-258.0	-230.7	-177.7	-230.7
10	$\text{CH}_3\text{TNH}_2^{2+} \rightarrow \text{CH}_2\text{TNH}_2^+ + \text{H}^+$	410.7	404.4	439.6	-136.9	-131.0	-115.3	-112.0	-105.2	-112.0
$\Delta(G_{11} - G_{10})$		124.9	92.4	144.5	118.6	72.5	142.7	118.7	72.5	118.6

Table 2 The predicted pKa values from the isodesmic reaction and G4(IEF-PCM) calculations. The reference experimental values are written in italic.

Reaction No.	Acid-base reaction	DMSO			water		
		<i>ortho</i>	<i>meta</i>	<i>para</i>	<i>ortho</i>	<i>meta</i>	<i>para</i>
a	$\text{ANH}_3^+ \rightarrow \text{ANH}_2 + \text{H}^+$		3.7 ⁱ⁾			4.6	
b	$\text{ANH}_2 \rightarrow \text{ANH}^- + \text{H}^+$		30.6			33.8 ⁱⁱ⁾	
c	$\text{ANH}_2^{*+} \rightarrow \text{ANH}^* + \text{H}^+$		6.4			7.0	
		<i>ortho</i>	<i>meta</i>	<i>para</i>	<i>ortho</i>	<i>meta</i>	<i>para</i>
1	$\text{CH}_3\text{TNH}_2 + \text{H}^+ \rightarrow \text{CH}_3\text{TNH}_3^+$	4.3	3.8	4.4	4.8	4.8	5.3
2	$\text{CH}_3\text{TNH}_2 \rightarrow \text{CH}_3\text{TNH}^- + \text{H}^+$	30.8	31.1	31.9	34.0	36.4	34.2
3	$\text{CH}_3\text{TNH}_3^+ \rightarrow \text{CH}_2\text{TNH}_3^{*+} + \text{H}^+$	32.4	35.6	36.8	35.8	39.5	36.4
4	$\text{CH}_3\text{TNH}_2 \rightarrow \text{CH}_2\text{TNH}_2^- + \text{H}^+$	43.7	43.9	47.7	46.9	47.1	47.1
5	$\text{CH}_3\text{TNH}^- \rightarrow \text{CH}_2\text{TNH}^{2-} + \text{H}^+$	53.7	51.0	55.8	56.3	53.6	59.4
6	$\text{CH}_2\text{TNH}_3^{*+} \rightarrow \text{CH}_2\text{TNH}_2^- + \text{H}^+$	4.9	1.4	4.6	8.3	4.7	8.3
7	$\text{CH}_2\text{TNH}_2^- \rightarrow \text{CH}_2\text{TNH}^{2-} + \text{H}^+$	40.8	38.3	40.0	43.9	40.9	46.5
8	$\text{CH}_3\text{TNH}_2^{*+} \rightarrow \text{CH}_3\text{TNH}^* + \text{H}^+$	6.7	7.0	7.2	7.3	7.6	7.3
9	$\text{CH}_3\text{TNH}_2^{*+} \rightarrow \text{CH}_2\text{TNH}_2^* + \text{H}^+$	6.1	6.5	7.1	6.7	7.1	6.7
10	$\text{CH}_3\text{TNH}_2^{2+} \rightarrow \text{CH}_2\text{TNH}_2^+ + \text{H}^+$	-38.6	-29.5	-39.9	-37.3	-28.0	-37.3
11	$\text{CH}_3\text{TNH}_2^{2+} \rightarrow \text{CH}_3\text{TNH}^+ + \text{H}^+$	-16.7	-17.8	-14.0	-16.5	-15.3	-16.5

i) Measured for aniline hydrochloride

ii) The value is estimated from experimental value for DMSO and theoretical values for water and DMSO